DEVELOPMENT AND ANALYSIS OF FRICTION MATERIAL FOR ECO-FRIENDLY BRAKE PAD USING SEASHELL COMPOSITE

Adebayo ADEKUNLE[1], Mojeed OKUNLOLA[1], Peter OMONIYI[1,2]*, Adekunle ADELEKE[3], Peter IKUBANNI[4], Tajudeen POPOOLA[1], Hassan IBRAHIM[1]

[1]Department of Mechanical Engineering, University of Ilorin, Ilorin 240003, Nigeria. adekunlebayo@yahoo.com, +2348033591465 (A.A.); mojeed_uthman91@yahoo.com, +2348132498155 (M.O.); omoniyi.po@unilorin.edu.ng, +2348135910454 (P.O.); tomtomleet@yahoo.co.uk, +2348063616248 (T.P.); ibrahim.kh@unilorin.edu.ng, +2347033973345 (H.I.)

[2]Department of Mechanical Engineering Science, University of Johannesburg, Johannesburg 2092, South Africa. 219126794@student.uj.za, +27622635779 (P.O.)

[3]Department of Mechanical Engineering, Nile University of Nigeria, Abuja 90001, Nigeria. adeleke.kunle@ymail.com, +2347035267800 (A.A.)

[4]Department of Mechanical Engineering, Landmark University, Omu-Aran 251101, Nigeria. ikubanni.peter@lmu.edu.ng, +2347065993936 (P.I)

*Corresponding author's email: omoniyi.po@unilorin.edu.ng

ABSTRACT

Asbestos has been banned in many countries as a result of its negative effects on the environment and human health. As a result, a human-friendly friction material is required to replace asbestos in brake pads. Hence, the powder metallurgy technique was undertaken to develop friction material from locally sourced asbestos-free materials. Seashell was used as base elements with other additives. The filler material considered had a particulate size of 300 µm, and epoxy resin was used as a binder. The produced brake pads were evaluated and compared to commercial brake pads in terms of their physical, mechanical, and tribological properties. According to the investigated properties of the developed brake pads, increasing the seashell content in the formulated brake pads resulted in a decrease in wear rate, and compressive strength. Water absorption, hardness, oil absorption, density, and thermal conductivity all varied differently at the same time. The coefficient of friction of the produced friction material ranges between 0.311 and 0.353. The results showed that seashell particles could effectively replace asbestos in producing friction material for brake pads in an automobile.

Keywords: Brake Pad, Composite, Epoxy Resin, Hardness, Sea Shell, Tensile Strength

1.0 INTRODUCTION

A brake acts as a mechanical device that prevents motion by absorbing the energy of a moving system [1–3]. It is used to slow or stop a moving vehicle's wheel, or to inhibit their motion, most commonly through friction [4]. For all vehicles equipped with brake discs, brake pads are an essential and important component of the disc braking system [5]. The brake pad uses pressure from the pedal through a fluid to the caliper containing the pads, forcing the friction material against the disc connected to the wheel. The wheel's rotation is altered by absorbing the kinetic energy of the wheel. The kinetic energy in the form of heat is dissipated to the surrounding [1,2].

Brake pads consist of four major materials: binders, fillers, friction materials, and reinforcements [3–6]. Friction materials play an important role in the brake system since the pad's crucial part decelerates and stops the wheel's rotation and is majorly made of composite materials [7,8]. In the past, asbestos was used as the frictional material in brake pads. However, because asbestos is now banned in many countries due to its carcinogenic nature, its use is discouraged [9,10]. Furthermore, at 200 ºC, the efficacy of the asbestos brake pad reduces [11]. Several researchers have replaced the carcinogenic asbestos-lined brake pads in the market with eco-friendly materials, such as palm kernel shells [12], periwinkle, sawdust, cow hooves, cow horn, bananas peels, and eggshell, together with other additives. However, one of the materials that have shown tremendous potential for friction material production is seashell. Seashell is an exoskeleton of an invertebrate composed of up to 96.8% calcium carbonate [13]. Seashells can be found at the reach of beaches in the United States, Australia, and the sub-region of Africa, where Nigeria is not excluded.

The use of palm kernel fiber as an asbestos replacement has been studied, and a replacement of up to 5% was found suitable for an excellent tribological property of brake pad [12]. In comparison, Bernard and Jayakumari [14] reported 8% palm fiber to give an optimum tribological property. Furthermore, the use of Areca sheath fiber has also been found suitable with 5% addition of Areca sheath having good tribological properties compared to higher percentage addition [15]. Generally, the use of alternative frictional materials has shown improved tribological properties over asbestos brake pads. Other materials which have been used in the manufacturing of brake pads are multiwall carbon nanotubes (MWCNT), Aluminum Magnesium alloys with Nickel Sulfate ($NiSO_4$) as filler materials have proved to

improve the tribological and mechanical properties of brake pads [4,16,17]. However, these materials come at a high price and are not readily available in the developing world.

As a result, the purpose of this article is to investigate the physicomechanical and tribological properties of brake pads made with seashells as frictional material and compare them to aftermarket products. The availability, cost of material, and properties are the primary considerations in choosing the materials for developing the brake pad.

2.0 Materials and method

The materials used in this study were seashell (friction material), palm kernel shell, and metal chips (reinforcement). Sawdust, charcoal (filler), and epoxy resin and hardener (Diethylenediamine)(binders). The seashells were collected from Eleko beach, Ajah Lagos State, Nigeria. The sawdust of teak (Tectona Grandis) wood was collected from Tanke sawmill, along University of Ilorin Road, Ilorin, while the palm kernel shell was collected from Iyeku, Odo-Otin South Local Government, Osun State. Metal chips of high carbon steel with a carbon content of 0.72% were collected from the Mechanical Engineering Department Central Laboratory, University of Ilorin, and were sieved with apertures of 1.7mm. Epoxy resin and hardener were purchased from the Ojota chemical market (Lagos), and charcoal was purchased at Gago junction, Tanke oke-odo, Ilorin.

The seashell, sawdust, palm kernel shell, and charcoal were sundried for three days (5 h/day) to remove excess moisture. They were then pulverized using a hammer mill and was sieved to a particle size of 300 µm, 300 µm, 300 - 150 µm, and 300 µm, respectively (Figure 1).

The samples in the proportion shown in Table 1 (seashell fines, sawdust fines, metal chips, palm kernel shell fines, and charcoal fines) were mixed thoroughly for homogeneity using a mechanical mixer at a speed of 600 rpm for ten minutes. The epoxy resin and hardener (2:1) were homogeneously mixed in a separate container. The mixtures were then blended to obtain a low moisture composition mixture. The blended mixture was transferred into a fabricated metallic mold. A force of 40 kN was applied to compress the material with a holding time of ten minutes under a hydraulic compression machine. The compression machine was then released, and the molded sample was ejected from the mold and left to dry at room temperature for 48 hours before transferring to an oven and cured for 60 minutes at 150 ^{o}C. As shown in Figure 2, the cured samples were cooled at room temperature and placed in a zip-locked bag for preservation before further analyses were carried out on them.

2.1 Density

The Archimedes' principle is used to calculate the volume and density of an irregularly shaped object by measuring its mass in air and practical volume when submerged in water. [5,18]. A small sample was cut off, and weight in air as W (g) and the same specimen was submerged in a graduated cylinder filled with water, and the volume of water displaced was recorded as V (cm^3). The density is expressed as shown in Equation 1 [18].

$$Density = \frac{W}{V} \quad (1)$$

Where W denotes weight of sample in air, V is volume of water displaced

The unit of density is g/cm^3.

2.2 Oil and Water Absorption

Oil and water absorption tests were carried out to determine the sample's vulnerability and porosity when submerged in water and oil for a specified period of time. In order to determine the absorption properties of the brake pad, Equation 2 was used. The oil used was SAE40 automotive engine oil. For 168 hours, the samples were immersed in water and oil (7 days). Specimens were removed from the water and oil, thoroughly cleaned to remove any remaining water and oil from the surfaces, and reweighed to determine the new weights recorded as W_f. Equation 2 was then used to calculate the percentage absorptions. [9,19,20].

$$\%Absorption = \frac{W_f - W_i}{W_i} \times 100 \quad (2)$$

where W_i is the weight before immersion and W_f is the weight after immersion.

2.3 Hardness Test

The hardness test was performed with the aid of Monsanto Testing Machine for hardness and shearing to determine the Brinell hardness of samples. The spherical indenter is 10.00 mm in diameter. Samples were cut to a specific size and were fixed into the tensiometer. A compression load of 1250 kg for 20 seconds was applied. The indented diameter was measured by eye scope [21]. Equation 3 is used to calculate the Brinell hardness (BHN) [22].

$$BHN = \frac{w}{\left(\frac{\pi D}{2}\right) \times \left(D - \sqrt{D^2 - d^2}\right)} \quad 3$$

Where *W* denotes the load on the indenter (kg), *D* denotes the diameter of the steel ball (mm), and *d* denotes the average measured diameter of the indentation (mm).

2.4 Abrasion Resistance/ Wear rate Test

An abrasion resistance test was carried using the pin-on-disc weight loss/wear test machine. A load of 20N was applied on the stylus pin for 200 cycles. After the cycle was completed, the sample was removed from the specimen holder and reweighed [9]. The specific wear rate is expressed in Equation 4, and the test was carried out according to ASTM G99 [16,23].

$$W_S = \frac{\Delta V}{F \times S} \quad 4$$

where *Ws* denotes the specific wear rate (mm^3/Nm), *V* denotes volume loss (mm^3), *F* the applied load (N), and *S* the sliding distance (m).

2.5 Friction Coefficient Test

An inclined plane was used to perform the coefficient of friction test. The standard specifies that the frictional coefficients of each sample be determined using an inclined angle (α) tilted and fixed at 40°. A small hole was made on the brake pads, and a thread of negligible weight was attached to the weighted sample (*F*) and was made to pass across the frictionless grooved pulley and connected to the weight hanger. The weight hanger's load was steadily increased until the pad slides at a constant velocity. The load was recorded as (*X*), and the coefficient of friction was calculated. The coefficient of friction computed using Equations 5 and 6 [24].

$$W = m \times a = m \times g \quad 5$$

Where *W* is weight of sample, *a* = *g* = acceleration due to gravity and *m* is mass of pad

$$\mu = \frac{X - F \sin \alpha}{F \cos \alpha} \quad 6$$

μ is the coefficient of friction

2.6 Thermal Conductivity Test

The Armfield Computer Compatible Linear Heat Conduction accessory HT11C was used for this experiment. The specimens were prepared to an average diameter of 30 mm diameter and 5 mm to accommodate the equipment.

2.7 Compression Strength Test

A compression test was also performed on the samples using a universal testing machine (Model: INSTRON 3369)[25,26]. All tests were carried out following ASTM D3410 [27].

2.8 Scanning Electron Microscopy (SEM) and Energy-dispersive X-ray fluorescence spectrometry (ED-XRF)

The distribution of the materials within the brake pad was determined using SEM analysis. The elemental composition of the composite was also determined using the ED-XRF.

3.0 Results and Discussion

3.1 Physico-mechanical and Tribological properties

Table 2 compares the properties of the developed composite brake pad to those of the market's existing brake pad. Table 3 also compares the physicomechanical and tribological properties of Sample D to the market's existing brake pad material, denoted as the control sample.

3.1.1 Density Assessment

Figure 3 depicts the density of the produced brake pads in comparison to the control sample. It was discovered that increasing the amount of seashell in the formulated samples resulted in a decrease in density. The decrease in density could be attributed to the low density of seashells, which increased the composition of the materials. They are lighter in weight and met the criteria of standard organization of Nigeria (SON) specifications. The density of the brake pads developed in this study are similar to what was reported by Popoola et al., [24] for brake pad produced using palm kernel shell, coconut shell, sea shell and cow bone. Lower density denotes higher quality than conventional friction material used in brake pad applications, as reported by Edokpia et al., [22].

3.1.2 Absorption Assessment

Figure 4 depicts the samples' percentages of water and oil absorption. Water and oil absorption decreased from sample A to sample E, indicating that the higher the seashell

content in the formulation, the less water and oil absorption. Sample E has the lowest water/oil absorption of 14.51/6.86 percent, while the control sample has 3.11/3.10 percent. The higher value of water and oil absorption of the produced samples can be attributed to the presence of voids in the samples and can be reduced by increasing the compressing force. Furthermore, the reduction in oil and water absorption as seashell content increases could be attributed to the impermeability nature of seashells. Also, the interfacial bonding energy provided by the binder contributed to the less porosity observed as the seashell content increases. This was also observed by Achebe et al., [6] who used palm kernel shell as filler material. Generally, all produced samples exhibited an improved water/oil absorption compared to that of the commercial sample.

3.1.3 Hardness Assessment

Figure 5 depicts the hardness behavior of the produced brake pads and the control sample. It was discovered that as the seashell content in the formulation increased, the hardness of the material increased uniformly. The hardness value obtained for each composite specimen is lower than that of the control friction material. The low hardness values obtained in all the produced samples could be attributed to decreased bonding strength and the intermolecular bonding within the composite material. The hardness value of the control friction material is 154.3 BHN, while the highest hardness value of the produced samples is 67.2 BHN and the lowest hardness was 6.3 BHN. These results were in line with reports of Achebe et al., [6], where an increase in palm kernel particles as a replacement of asbestos increased hardness.

3.1.4 Wear (Abrasion) Resistance Assessment

The specific wear rate of composite specimens and the control sample is depicted in Figure 6. The specific wear rate of specimens was found to decrease as the seashell content increased and could be attributed to the high hardness of seashells. Furthermore, the calcium carbonate present in the seashell act as a binding material just like cement, thereby improving the wear rate of the composite [13]. Also, Park et al., [28] attributed resistance to the wear of seashells to the film formed by carbon carbonate. The specific wear rate decreased from sample B to D, with hardness values ranging from 15.6 to 57.4 BHN and specific wear rates ranging from 0.497 to 0.0831. The specific wear rate of the control sample is 0.0812 with a hardness value of 154.3 BHN. The increase in seashell content resulted in a corresponding decrease in the effectiveness of binder binding the composite under the compressive force of 40 kN. Sample

D demonstrates the best friction material composition because it has the highest wear resistance of all the samples produced. The sliding distance is critical in determining the specific wear rate, as a greater sliding distance results in a lower wear rate. The equivalent specific wear rate at the same sliding distance revealed that the specific wear rate of sample D at the same sliding distance has greater wear resistance than the control brake pad material. Sample D has a specific wear rate of 0.0614, which is 32.25 percent higher than the control sample, which has a specific wear rate of 0.0812. The results show that the specific wear rates of sample D outperform the control sample. Furthermore, the Archard wear model [17] stipulates that the volume of material removal is inversely proportional to the hardness of the material and was further corroborated by Ezekiel and Inambao [29]. This phenomenon was observed in the brake pad material, where the higher hardness of the control sample resulted in a lower wear rate of the sample.

3.1.5 Coefficient of Friction Assessment

Figure 7 presents the coefficient of friction of produced brake pads and the control brake pad. It is shown that samples A, C, and E have the same coefficient of friction (μ) of 0.35, and samples B and D have the μ= 0.311 and 0.315, respectively. These results could be attributed to the distribution of seashells in the samples. From the results, it can be deduced that sample D (μ= 0.315) has the closest coefficient of friction to the control sample (μ= 0.318). The competitive friction performance could further be ascribed to the improved hardness, the seashells addition, and the bonding strength the binder added [22]. Generally, the coefficient of friction performance was similar to that of brake pads produced with palm kernel fibers ranging between 0.325-0.365 [12].

3.1.6 Thermal Conductivity Assessment

From Figure 8, it could be generalized that thermal conductivity increases as the seashell content of the produced brake pad increase from sample B to E. The drop in thermal conductivity value at sample D is due to the optimum and proper arrangement of particles, which makes the sample less porous. The highest thermal conductivity of sample E is due to the oversaturation of the seashell in the composite, which is attributed to higher heat absorption [28]. The thermal conductivity of the control brake pad is 3.161 W/m^{o}C, while the thermal conductivity of specimen D is 2.799 W/m^{o}C. As a result, specimen D has a higher heat resistance than the control sample. The thermal conductivity of maize-husk-based friction material was in the range of 0.251 – 0.372 W/mK for most agro-residue-based

friction material developed as obtained from literature. The cocoa-beans-shell-base brake pad was between 0.239 – 0.338, and the palm kernel shell-based friction material (1.460 W/mK) was reported by Dagwa and Ibhadode [30]. The results show the seashell base brake pad will compete favourably with the existing non-abestors based brake pads. The favourable competition with other brake pads could also be attributed to little or no cracks or voids attributed to thermal stress due to cyclic heating and cooling of the brake pads during wear test [31].

3.1.7 Compressive assessment

It is observed from Figure 9 that the compressive strength of the produced brake pads decreased as the seashell content increased from samples A to E. This shows that the brittleness of the produced brake pads increased as seashell content increased, resulting in a decrease in the energy required to break the specimen. The higher compressive extension at failure of sample D is attributed to a proper and homogeneous arrangement of particles in the sample. The compressive stress, extension, and energy at break of the sample D are 17.74132 MPa, 1.96356 mm, and 6.90480 J, respectively, while the control friction material is 13.83705 MPa, 2.22931 mm, and 5.44598 J.

3.1.8 Scanning electron microscope and XRF analysis

Figure 10 shows the arrangement of particle distribution in the produced friction material and the control sample. Most of the dark sides from figure 10a and 10b show the presence of carbon, silicon, and some iron. Silicon carbide is known to be one of the hardest materials. Therefore, this is attributed to the hardness of the material [32]. The white areas are majorly calcium carbonate and iron, as also observed in [1]. Calcium carbonate has also been attributed to reducing shrinkage during composite molding. It is also advantageous as it has a lower weight and high melting point of 850 °C [32], microfilm formation by $CaCO_3$ also improves the wear resistance of the brake pad composite [28]. The significant elements found in the materials are presented in Table 4. The particle arrangement in the composite friction materials increased hardness as the seashell particle in the samples increased.

4.0 Conclusion

The results demonstrated that seashells have the properties required to produce friction material for brake pads due to the similarity of their performance to that of a commercially

produced brake pad. The hardness, wear resistance, and compressive strength of the produced sample are all important factors in brake pad production, and sample D performed admirably. Increased seashell content in the formulation resulted in a decrease in sample density, water absorption, oil absorption, and thermal conductivity.

The findings of this study indicated that seashell, in conjunction with additives, could be used effectively as a replacement for asbestos-lined friction material for brake pads with no known health consequences.

Conflicts of interest: None declared

Authors' contributions

AA (Adebayo Adekunle); MO; AA (Adeleke Adekunle); PI; PO; supervision and writing. AA (Adebayo Adekunle); MO; AA (Adeleke Adekunle); PI; PO; project planning and design. MO; PO; AA (Adebayo Adekunle) experimentations. TP; HI; PO; AA (Adeleke Adekunle); PI analyzes and interpretation. AA (Adebayo Adekunle); HI; TP; AA (Adeleke Adekunle); PI; revision. All authors contributed to the scientific discussion and approved the final manuscript.

Funding Statement

No funding was received for this research.

Acknowledgements

Not applicable.

References

[1] Elzayady, N. and Elsoeudy, R. "Microstructure and wear mechanisms investigation on the brake pad", J. Mater. Res. Technol., 11, pp. 2314–2335 (2021).

[2] Kumar, S. and Ghosh, S.K. "Particle emission of organic brake pad material : A review", J. Automob. Eng., pp. 1–11 (2019).

[3] Maleque, M.A., Atiqah, A., Talib, R.J., et al., "New Natural Fibre Reinforced Aluminium Composite for Automotive Brake Pad", Int. J. Mech. Mater. Eng., 7, pp. 166–170, (2012).

[4] Kumar, S. and Ghosh, S.K. "Porosity and tribological performance analysis on new developed metal matrix composite for brake pad materials", J. Manuf. Process., 59, pp. 186–204 (2020).

[5] Singh, T. and Patnaik, A. "Performance assessment of lapinus – aramid based brake pad hybrid phenolic composites in friction braking", Arch. Civ. Mech. Eng., 5, pp. 151–161 (2014).

[6] Achebe, C.H. Chukwuneke, J. and Anene, F.A. "A retrofit for asbestos-based brake pad employing palm kernel fiber as the base filler material", J. Mater. Des. Appl., pp. 1–8. (2018).

[7] Mausam, K. Sharma, A. and Singh, P.K. "Materials Today : Proceedings Calculating

stress , temperature in brake pad using ANSYS composite materials", Mater. Today Proc., 45, pp. 3547–3550 (2021).

[8] Ozdemir, A.O. and Karata, C. "Experimental determination of fracture toughness of woven / chopped glass ber hybrid reinforced thermoplastic composite laminates", Sci. Iran., 28, pp. 2202–2212 (2021).

[9] Pujari, S. and Srikiran, S. "Experimental investigations on wear properties of Palm kernel reinforced composites for brake pad applications", Def. Technol., 15 pp. 295–299 (2019).

[10] Lawal, S.S. Bala, K.C. and Alegbede, A.T. "Development and production of brake pad from sawdust composite", Leonardo J. Sci., pp. 47–56 (2017).

[11] Sukrawan, Y. and Mardani, S.A. "Effect of Bamboo Weight Faction on Mechanical Properties in Non-Asbestos Composite of Motorcycle Brake Pad", Mater. Phys. Mech., 42, pp. 367–372 (2019).

[12] Krishnan, G.S. Babu, L.G. Pradhan, R. et al., "Study on tribological properties of palm kernel fiber for brake pad applications Study on tribological properties of palm kernel fi ber for brake pad applications", Mater. Res. Express., 7, (2020).

[13] Bin Wan Mohammad, W.A.S. Othman, N.H. Wan Ibrahim, M.H. et al., "A review on seashells ash as partial cement replacement", IOP Conf. Ser. Mater. Sci. Eng., 271 (2017).

[14] Bernard, S.S. and Bernard, S.S. "Pressure and temperature sensitivity analysis of palm fiber as a biobased reinforcement material in brake pad", J. Brazilian Soc. Mech. Sci. Eng. 40, pp. 1–12 (2018).

[15] Krishnan, G.S. Jayakumari, L.S. Babu, L.G. et al., "Investigation on the physical , mechanical and tribological properties of areca sheath fibers for brake pad applications, Mater. Res. Express., 6 (2019).

[16] Kumar, S. and Ghosh, S.K. "Statistical and artificial neural network technique for prediction of performance in AlSi10Mg-MWCNT based composite materials", Mater. Chem. Phys., 273(125136), (2021).

[17] Kumar, S. and Ghosh, S.K. "Statistical and computational analysis of an environment-friendly MWCNT / NiSO4 composite materials", J. Manuf. Process., 66, pp. 11–26 (2021).

[18] Aweda, J.O. Omoniyi, P.O. and Ohijeagbon, I.O. "Suitability of Pulverized Cow Bones as a Paving Tile Constituent", 2nd Int. Conf. Eng. a Sustain. World, IOP Conference Series, Ota, 012046, (2018).

[19] Ohijeagbon, I.O. Adekunle, A.S. Omoniyi, P.O. et al., "Impact of Production Methods on Some Engineering Properties of Interlocking Tiles", Adeleke Univ. J. Eng. Technol., 2, pp. 99–108 (2019).

[20] Elakhame, Z.U. Jimoh, S.O. and Bankole, L.K. "Production and Characterization of Asbestos Free Brake Pads From Kenaf Fiber Composite", Adeleke Univ. J. Eng. Technol., 3, pp. 69–78 (2020).

[21] Omoniyi, P.O. Ohijeagbon, I.O. Aweda, J.O. et al., "Investigation of Brinell Hardness and Compressive Strength of Pulverized Cow Bones and Lateritic Paving Tiles", Adeleke Univ. J. Eng. Technol., 1, pp. 59–69 (2018).

[22] Edokpia, R.O. Aigbodion, V.S. Atuanya, C.U. et al., "Experimental study of the

properties of brake pad using egg shell particles–Gum Arabic composites", J. Chinese Adv. Mater. Soc., 4, pp. 172–184 (2016).

[23] ASTM G99, "Standard Test Method for Wear Testing with a Pin-on-Disk Apparatus 1", Astm Int., 05, pp. 1–6 (2017).

[24] Popoola, O.T. Rabiu, A.B. Ibrahim, H.K. et al., "Production of Automobile Brake Pads from Palm Kernel Shell , Coconut Shell , Seashell and Cow Bone", Adeleke Univ. J. Eng. Technol., 4, pp. 92–101 (2021).

[25] Omoniyi, P. Ohijeagbon, I. Aweda, J. et al., "Experimental data on the compressive and flexural strength of lateritic paving tiles compounded with pulverized cow bone", Data Br., 33, pp. 4–11 (2020).

[26] Omoniyi, P.O. Aweda, J.O. Ohijeagbon, I.O. et al., "Modeling and Simulation of Mechanical Properties of Pulverized Cow Bone and Lateritic Paving Tiles", Stavební Obz. - Civ. Eng. J., 29, pp. 551–558 (2020).

[27] ASTM D3410/D3410M, "Standard Test Method for Compressive Properties of Polymer Matrix Composite Materials", ASTM Int., 03, pp. 1–13 (2016).

[28] Park, J. Gweon, J. Seo, H. et al. "Effect of space fillers in brake friction composites on airborne particle emission : A case study with BaSO 4 , Ca (OH) 2 , and CaCO 3", Tribol. Int., 165(107334), (2022).

[29] Ezekiel, I.O. and Inambao, F. "The Effect of Carbon Nanospheres on the Properties of Bio-Based Hybrid Nanocomposite Brake Pad Materials", Int. J. Mech. Prod., 11, pp. 37–52 (2021).

[30] Ibhadode, A.O.A. and Dagwa, I.M. "Development of asbestos-free friction lining material from palm kernel shell", J. Brazilian Soc. Mech. Sci. Eng., 30, pp. 166–173 (2008).

[31] Borawski, A. "Testing Passenger Car Brake Pad Exploitation Time ' s Impact on the Values of the Coefficient of Friction and Abrasive Wear Rate Using a Pin-on-Disc Method", Materials (Basel)., 15, pp. 1–16 (2022).

[32] Kumar, V.V. and Kumaran, S.S. "Friction material composite : types of brake friction material formulations and effects of various ingredients on brake performance – a review", Mater. Res. Express., 6, pp. 1–15 (2019).

Nomenclature

μ = coefficient of friction

$a = g$ = acceleration due to gravity (m/s^2)

Figure 1

Figure 2

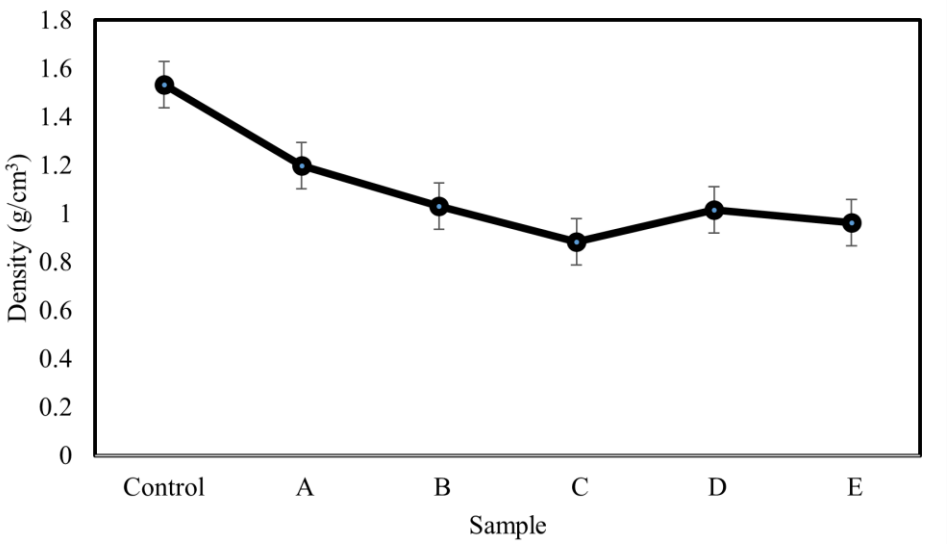

Figure 3

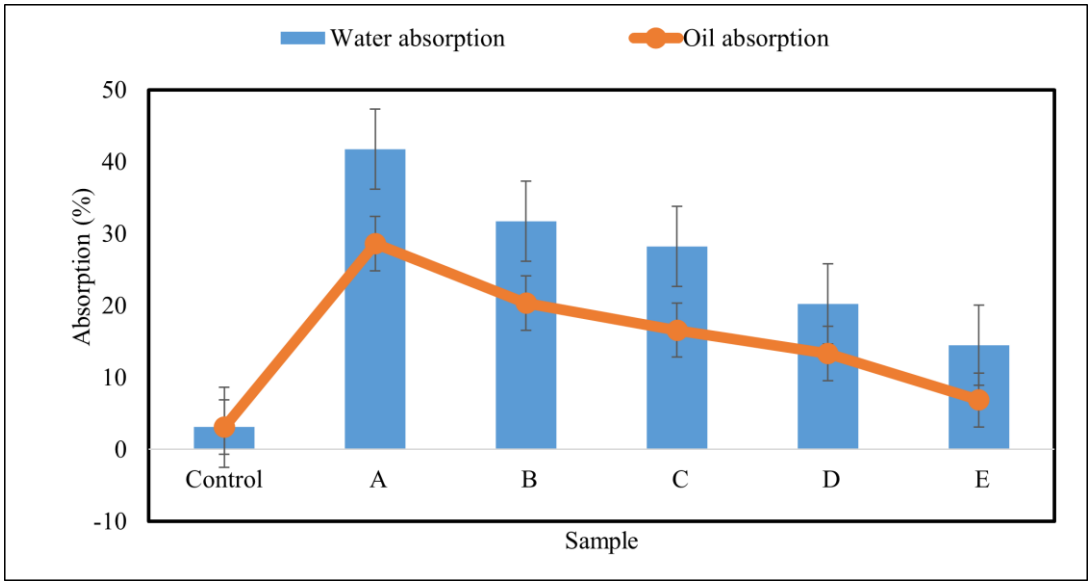

Figure 4

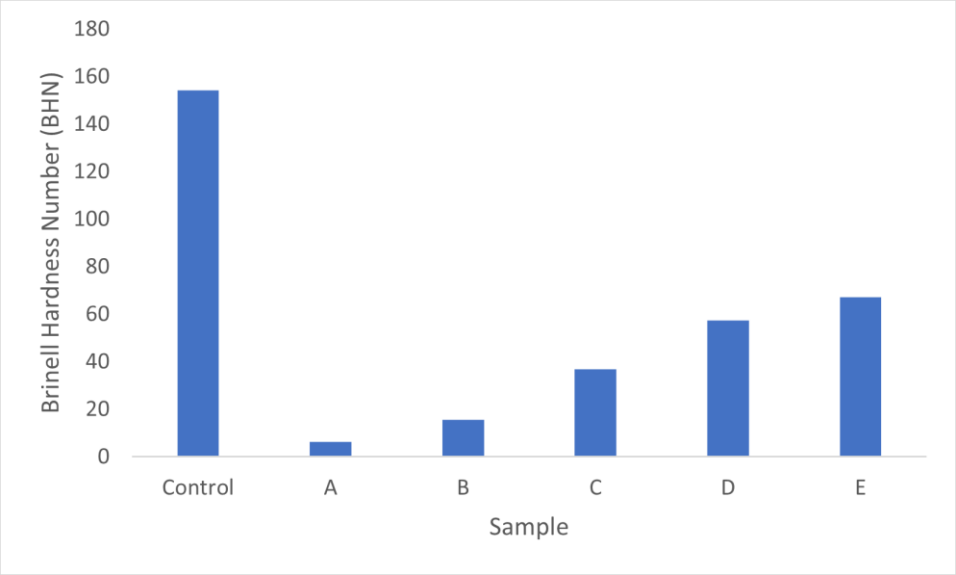

Figure 5

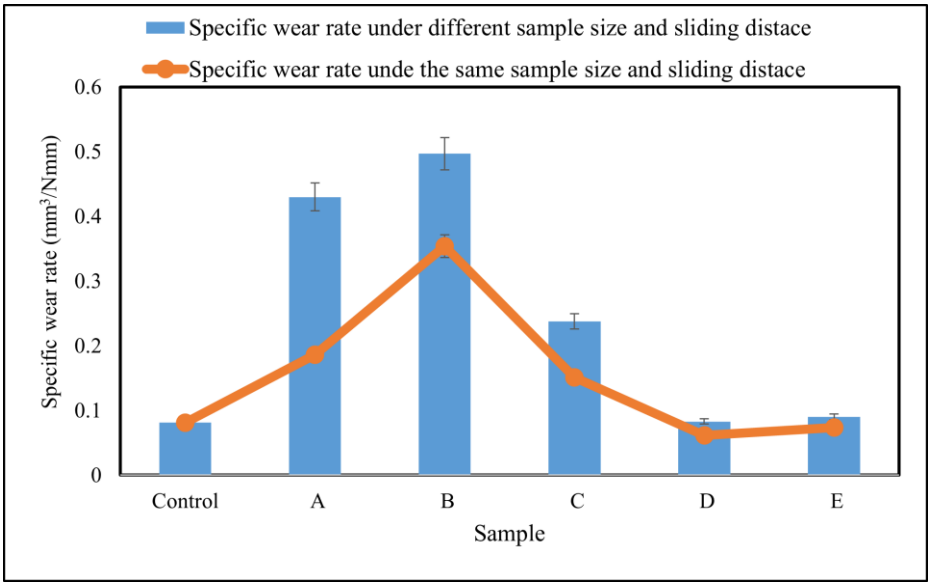

Figure 6

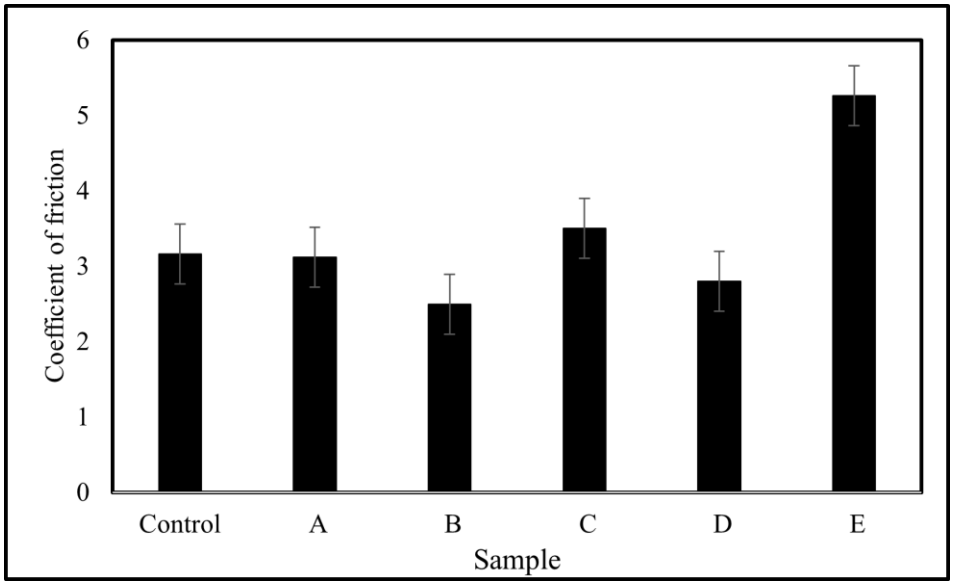

Figure 7

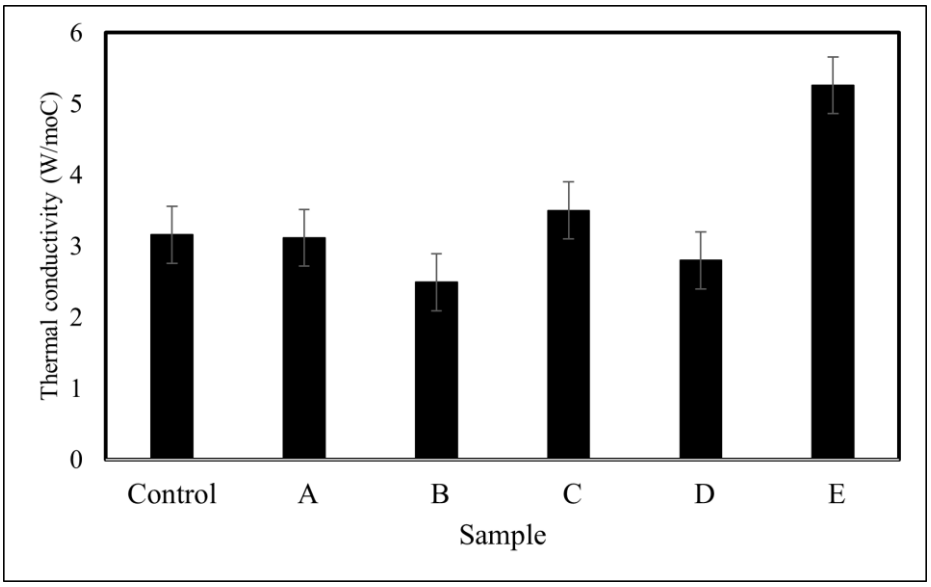

Figure 8

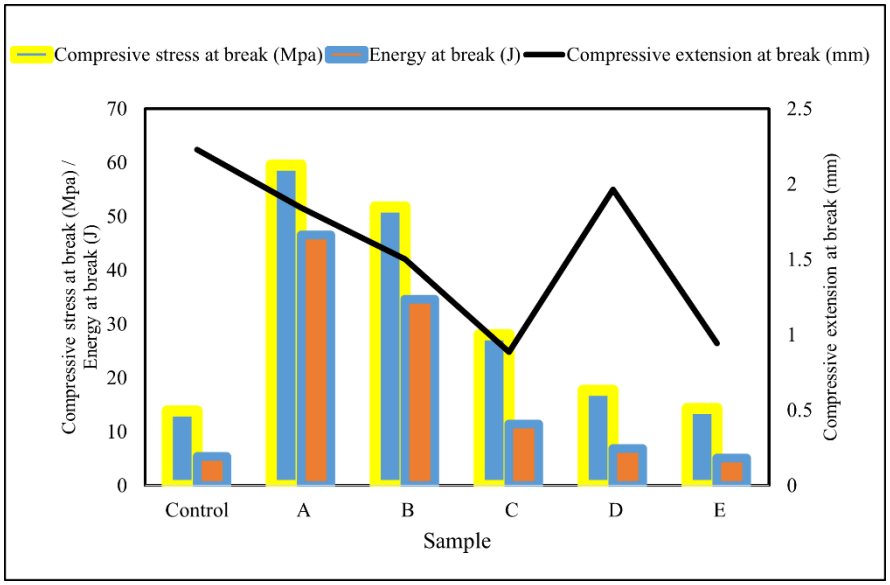

Figure 9

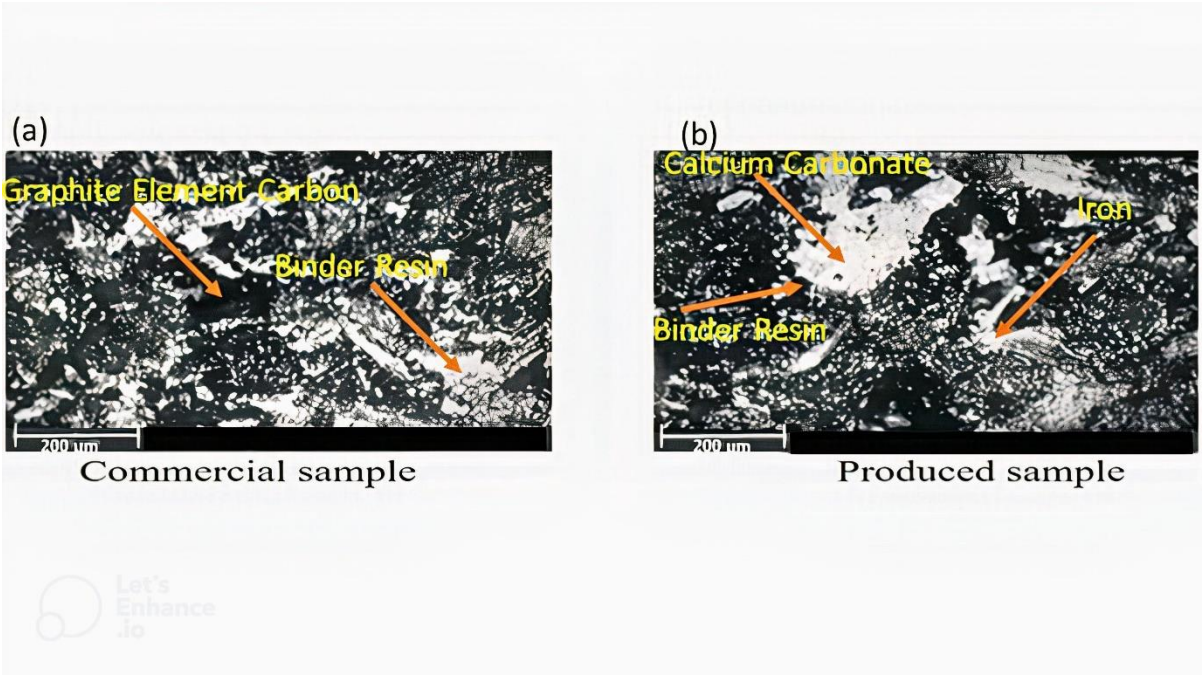

Figure 10

Table 1

Sample	Seashell (g)	Sawdust (g)	Palm kernel shell (g)	Charcoal (g)	Metal chips (g)	Binder (g)	Total (%)
A	15	35	3	10	10	27	100
B	20	30	5	8	10	27	100
C	25	25	7	6	10	27	100
D	30	20	9	4	10	27	100
E	35	15	11	2	10	27	100

Table 2

Sample/property	A	B	C	D	E	Control
Density (g/cm^3)	1.198	1.030	0.884	1.015	0.962	1.533
Water absorption (%)	41.7700	31.7680	28.2230	20.2470	14.5140	3.113
Oil absorption (%)	28.6170	20.3350	16.5940	13.326	06.8630	3.103
Hardness (BHN)	6.3	15.6	36.9	57.4	67.2	154.3
Specific wear rate (mm^3/Nm)	0.186	0.354	0.151	0.0614	0.0740	0.0812

COF	0.351	0.311	0.352	0.315	0.353	0.318
Thermal conductivity (W/m^oC)	3.118	2.494	3.501	2.799	5.261	3.161
Compressive strength (MPa)	59.52491	51.73037	28.00349	17.74132	14.32324	13.837

Table 3

Property	Control sample	Produced sample
Density (g/cm^3)	1.533	1.015
Water absorption (%)	3.113	20.247
Oil absorption (%)	3.103	13.326
Hardness (BHN)	154.3	57.4
Specific wear rate (mm^3/Nm)	0.0812	0.0614
Coefficient of friction	0.318	0.315
Thermal conductivity (W/m^oC)	3.161	2.799
Compressive strength (MPa)	13.837	17.741

Table 4

Element	% wt in sample A	% wt in sample D	% wt in sample E	% wt in sample Control
Fe	66.634	59.230	67.552	88.759
C	5.715	7.016	5.959	4.990
Ag	3.083	3.556	3.473	<LOD
Ca	2.723	5.012	2.041	2.010
Pd	3.536	3.087	2.133	<LOD
Si	3.558	6.712	4.116	<LOD

Cd	5.093	5.351	4.949	<LOD
O	8.243	10.032	7.918	2.981
Co	1.415	<LOD	1.859	0.594
Cr	<LOD	<LOD	<LOD	0.576
Pb	<LOD	<LOD	<LOD	0.0905

Biographies

Adebayo Adekunle (Ph.D.) is a lecturer at the Department of Mechanical Engineering, University of Ilorin, Nigeria. His research works are in mechanical design, fabrication, and production engineering. He is a registered professional engineer with the Council for the Regulation of Engineering in Nigeria (COREN).

Mojeed Okunlola completed his master's degree at the Department of Mechanical Engineering, University of Ilorin. His research interests include composite engineering, simulation, and modeling of composite materials.

Peter Omoniyi (Ph.D.) is a lecturer at the Department of Mechanical Engineering, University of Ilorin. He is a registered professional engineer with the Council for the Regulation of Engineering in Nigeria (COREN). He has published several articles in the area of composite engineering, fusion welding, and additive manufacturing.

Adekunle Adeleke (Ph.D.) is a lecturer at the Nile University of Nigeria, Abuja, Nigeria. He is a registered professional engineer with the Council for the Regulation of Engineering in Nigeria (COREN). He is a prolific researcher and has published several articles in the field of composite engineering.

Peter Ikubanni (Ph.D.) is currently a lecturer at the Department of Mechanical Engineering, Landmark University, Nigeria. He is a registered professional engineer with the Council for the Regulation of Engineering in Nigeria (COREN). He has authored several publications in the area of composite engineering.

Tajudeen Popoola (Ph.D.) is currently a lecturer at the Department of Mechanical Engineering, University of Ilorin. He is a registered professional engineer with the Council for the Regulation of Engineering in Nigeria (COREN). He has authored several articles in the area of composite engineering, simulation, and modeling of engineering problems.

Hassan Ibrahim is a lecturer at the Department of Mechanical Engineering, University of Ilorin. He is a registered professional engineer with the Council for the Regulation of

Engineering in Nigeria (COREN). His major research focus is in the area of material characterization and composite engineering.